Figure S1

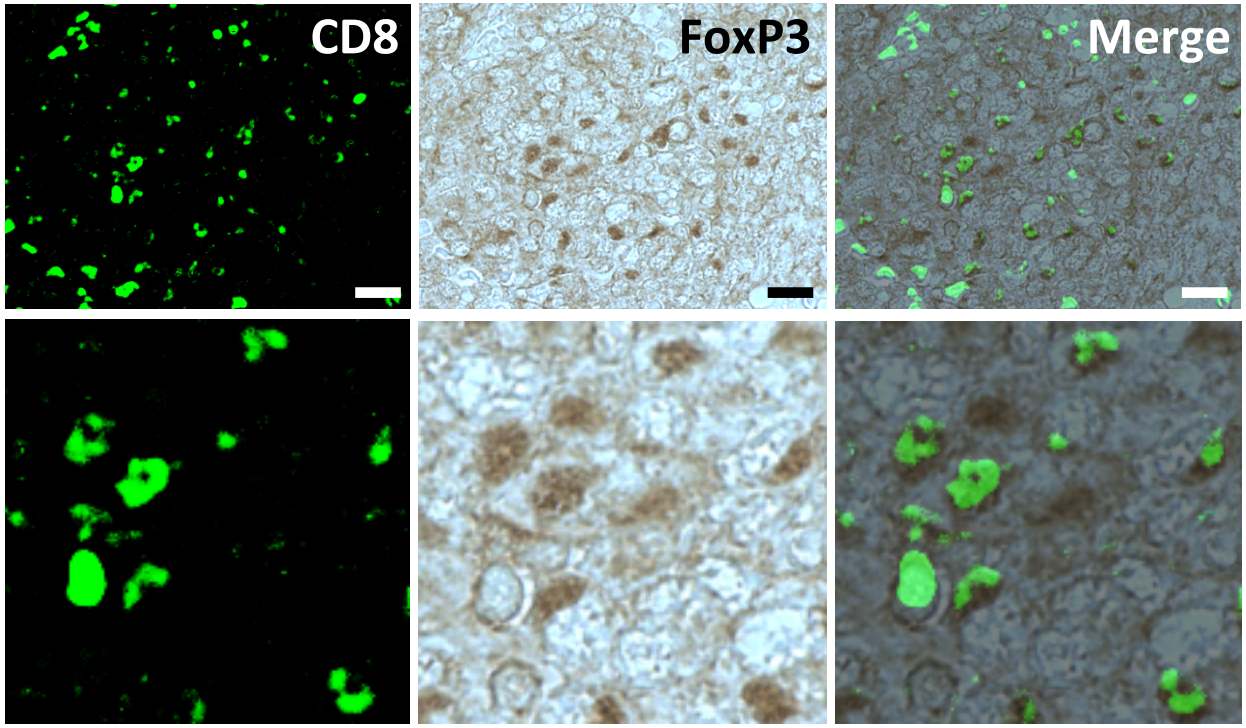

Localization of CD8 Tregs in human lymph nodes

Frozen section from human lymph nodes were dual-stained with anti-CD8 (left panels) and anti-FoxP3 (middle panels). Bound anti-CD8 antibodies were visualized by immunofluorescence and anti-FoxP3 antibodies by immunohistochemistry. Merged images (right panels) demonstrate $CD8^{+}FoxP3^{+}$ T cells within the T-cell rich zones. Images are representative for 5 different tissues. Scale bar 20 µm.

Figure S2

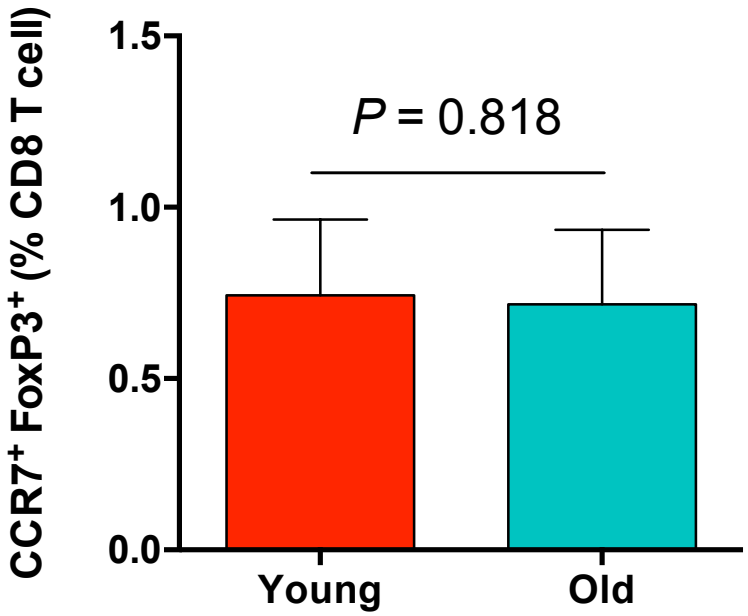

Comparable frequencies of $CD8^+CCR7^+FoxP3^+$ T cells in young and old persons

Frequency of $CD8^+CCR7^+FoxP3^+$ Tregs in peripheral blood of young and old donors were analyzed by flow cytometry. Results are shown as mean ± SD from 7 independent experiments.

Figure S3

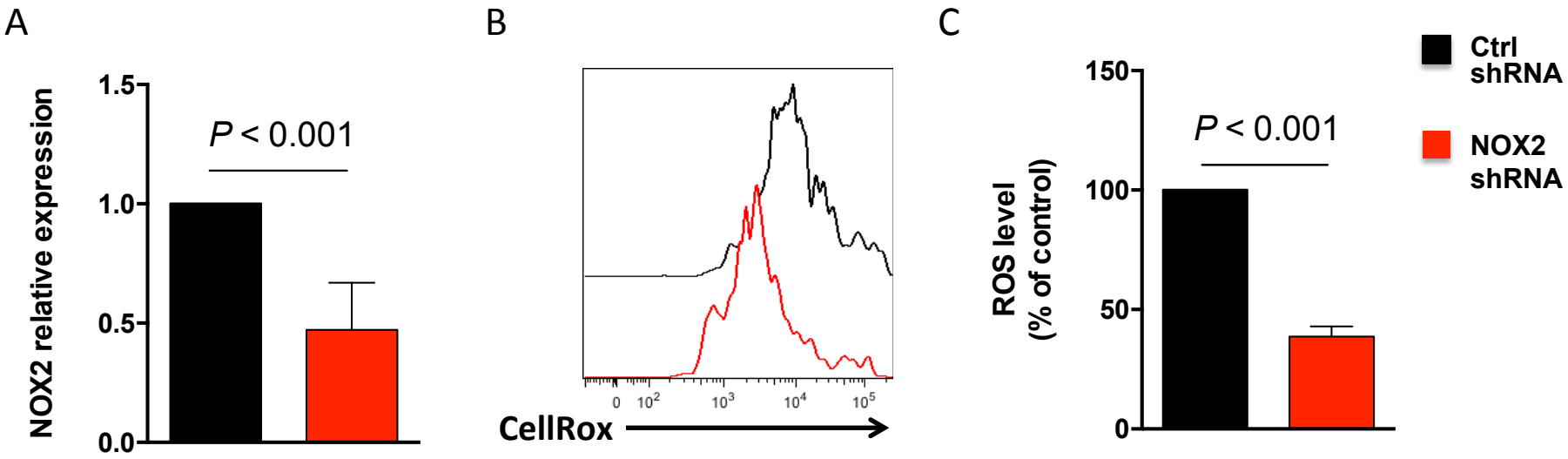

Partial NOX2 knockdown results in partial reduction of ROS production

(A) CD8 Tregs were transfected with NOX2 shRNA or control shRNA for 24h, and analyzed for NOX2 expression by qPCR. Mean ± SD of relative NOX2 expression from 5 independent experiments.

(B, C) Transfected cells were loaded with the ROS-sensitive probe CellRox and intracellular ROS levels were measured by flow cytometry. Representative histograms and summary of 4 independent experiments (mean ± SD) are shown.

Figure S4

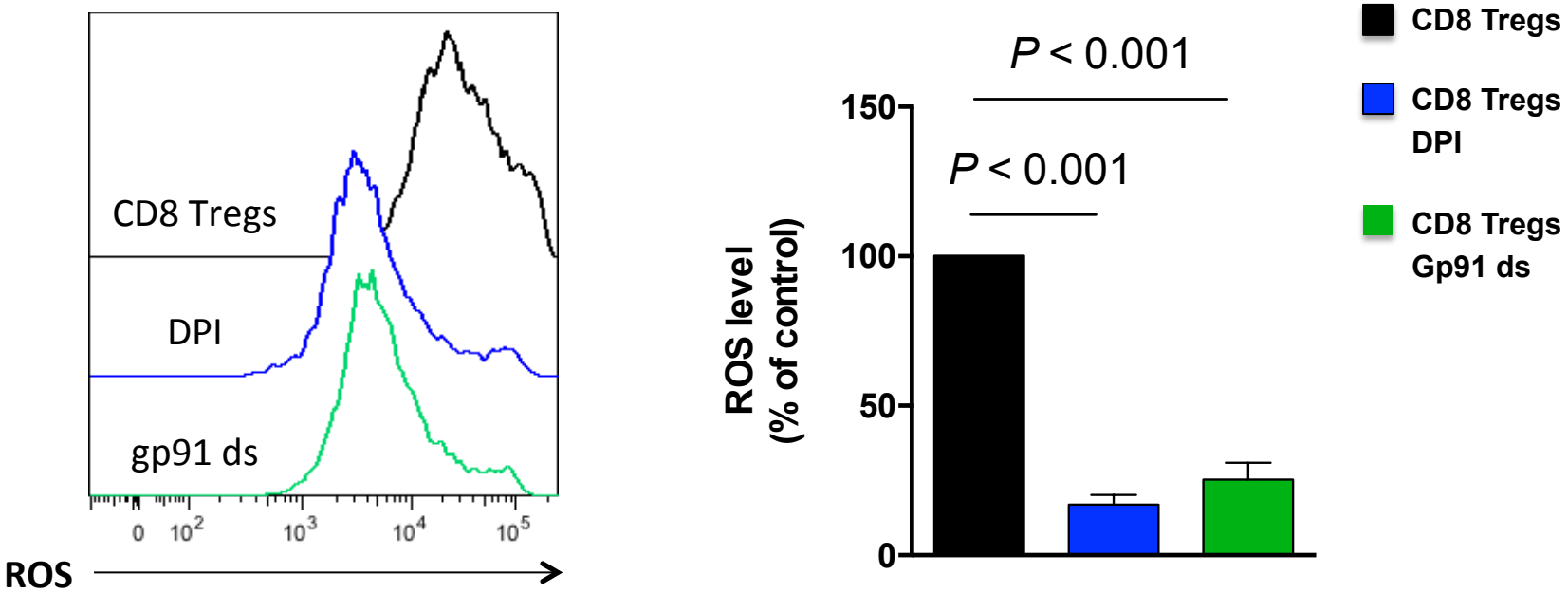

ROS production in CD8 Tregs

CD8 Tregs were left untreated or pretreated for 20h with DPI or Gp91 ds-tat. Cells were loaded with CellROX to measure cellular ROS levels. Untreated CD8 Tregs served as controls. Representative histograms and summary of 5 independent experiments (mean ± SD) are shown.

Figure S5

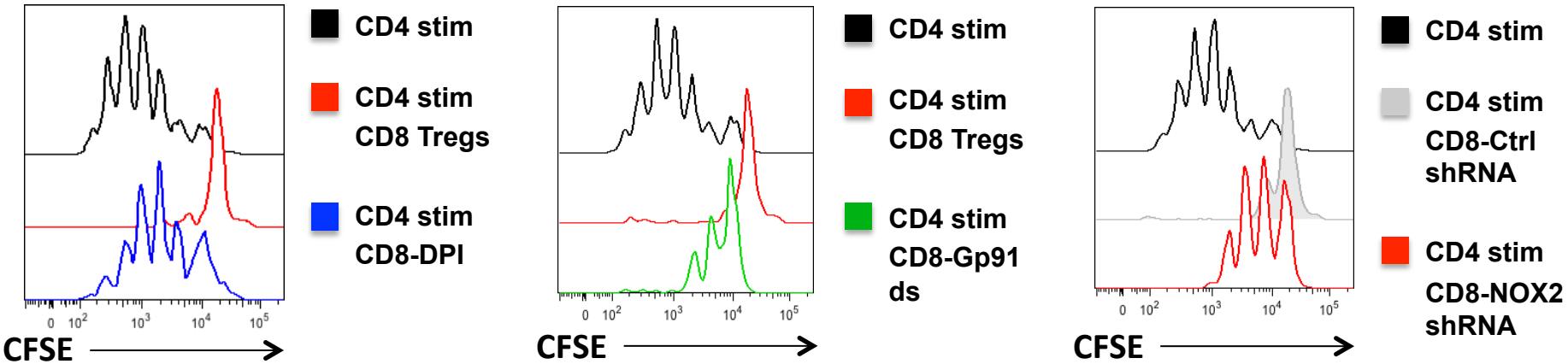

Interfering with NOX2 function abrogates the suppressive activity of CD8 Tregs

CD8 Tregs were pretreated with DPI, Gp91 ds-tat or NOX2 knockdown, respectively, and subsequently tested for their suppressive function. CD4 T cells were labeled with CFSE, incubated with or without CD8 Tregs (1:1 ratio) and stimulated with anti-CD3/CD28 beads for 4 days. CD4 T cell proliferation was quantified by assessing CFSE dilution with flow cytometry. One representative dataset from 3 independent experiments is shown.

Figure S6

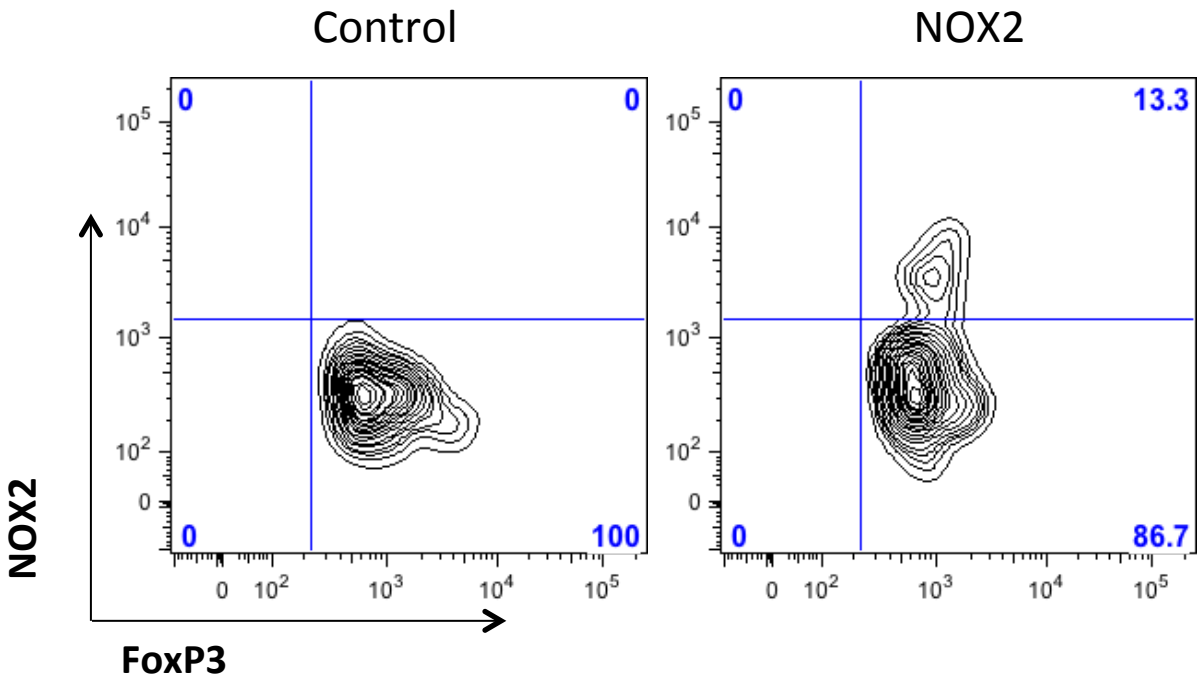

Expression of NOX2 on CD4 Tregs in healthy individuals

Cellular expression of NOX2 was analyzed in gated $CD4^{+}FoxP3^{+}$ T cells in the peripheral blood of healthy donors. FMO served as control. A representative result from one of 6 individuals is shown.

Figure S7

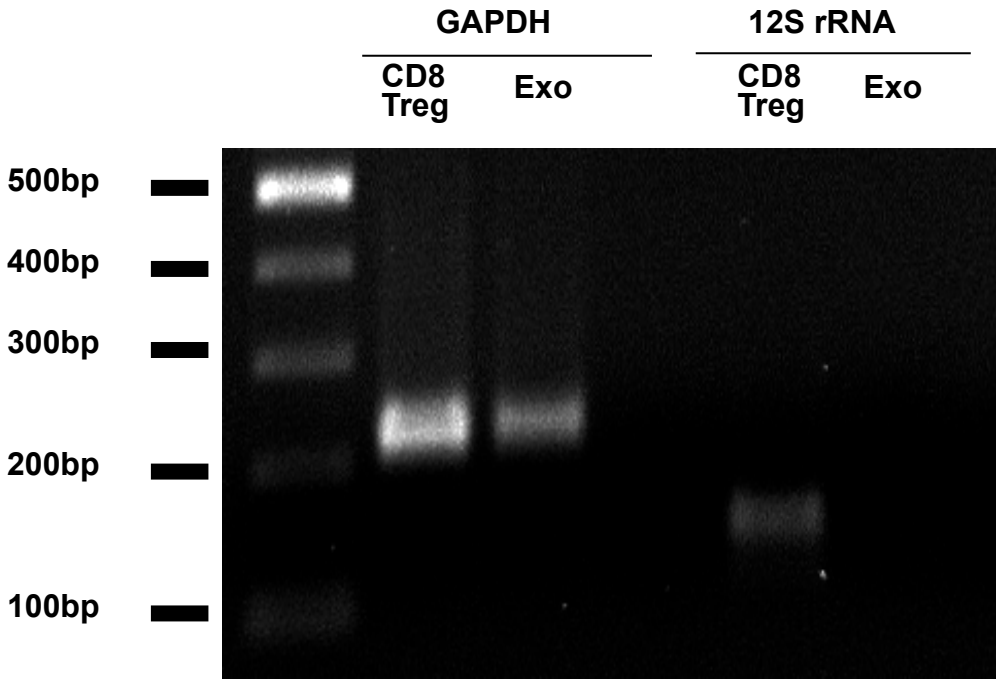

Mitochondrial 12S rRNA is not expressed in CD8 Treg-derived exosomes.

DNA was extracted from CD8 Tregs and from CD8-Treg-derived exosomes (Exo). GAPDH- and 12S rRNA-specific sequences were amplified by PCR and electrophoresed on an agarose gel.

Figure S8

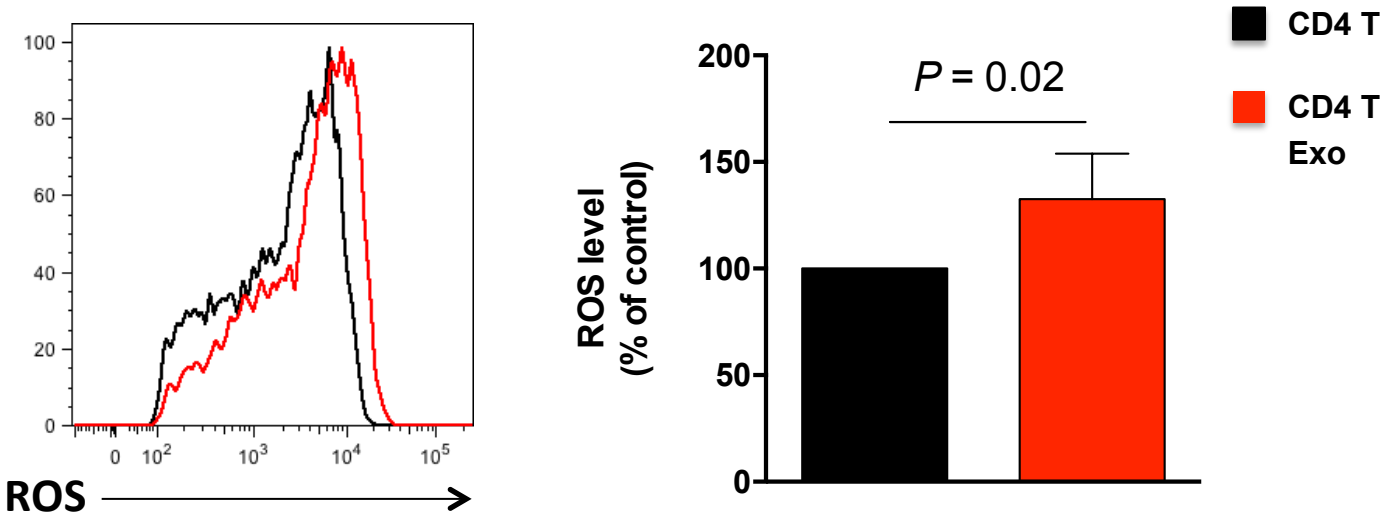

CD8 Treg-derived exosomes increase ROS levels in CD4 T cells

CD4 T cells were incubated with CD8 Treg-derived exosomes (1:2500 ratio) for 60 min and then loaded with CellROX to detect ROS levels. Untreated CD4 T cells were used as controls. Representative histograms and summary of 4 independent experiments (mean ± SD) are shown.

Figure S9

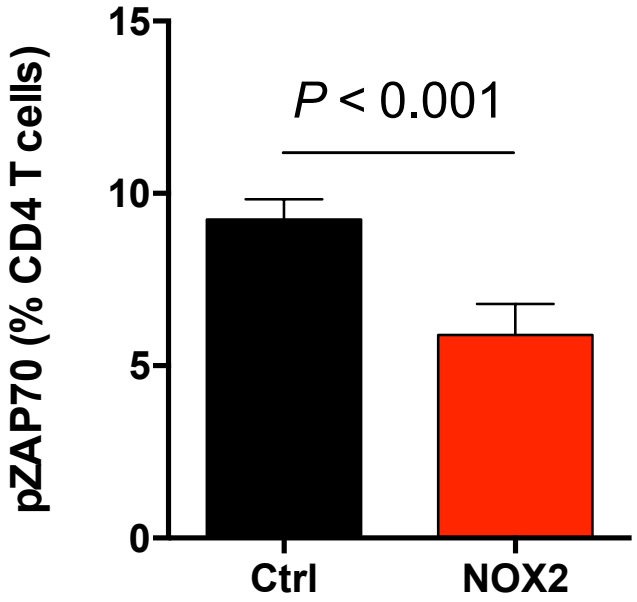

Overexpression of NOX2 in CD4 T cells suppresses membrane-proximal signaling

CD4 T cells were transfected with a control or NOX2 expression vector, stimulated with anti-CD3/CD28 beads (1:1) for 10min, and analyzed for ZAP70 phosphorylation. Results are shown as mean ± SD from 5 independent experiments.